PUBLICATIONS OF THE ASTRONOMICAL SOCIETY OF THE PACIFIC, **114**:656–670, 2002 June

Stellar Variability in a Survey of Field Stars

MARK E. EVERETT[1] AND STEVE B. HOWELL[1]

Astrophysics Group, Planetary Science Institute, 620 North 6th Avenue, Tucson, AZ 85705; everett@psi.edu, howell@psi.edu

GERARD T. VAN BELLE

Jet Propulsion Laboratory, California Institute of Technology, 4800 Oak Grove Drive, Pasadena, CA 91109; gerard@huey.jpl.nasa.gov

AND

DAVID R. CIARDI

Department of Astronomy, University of Florida, 211 Bryant Space Sciences Building, Gainesville, FL 32611; ciardi@astro.ufl.edu

Received 2001 December 10; accepted 2002 February 25

ABSTRACT. We present results from a 5 night wide-field time-series photometric survey that detects variable field stars. We find that the fraction of stars whose light curves show variations depends on color and magnitude, reaching 17% for the brightest stars in this survey ($V \sim 14$) for which the photometric precision is best. The fraction of stars found to be variable is relatively high at colors bluer than the Sun and relatively low at colors similar to the Sun and increases again for stars redder than the Sun. We present light curves for a sample of the pulsating and eclipsing variables. Most of the stars identified as pulsating variables have low amplitudes ($\Delta V = 0.01$–0.05), relatively blue colors, and multiple periods. There are 13 stars we identify as either SX Phoenicis or δ Scuti stars. These classes represent a significant contribution to the total number of blue variables found in this survey. Another 17 stars are identified as eclipsing variables, which have a wide range in color, magnitude, and amplitude. Two variable giants are observed, and both show night-to-night ~1% variations. We present data for 222 variables in total, most of which are not classified. Implications of surveys for stellar variability and interferometry are briefly discussed.

1. INTRODUCTION

Stellar photometry reveals classes of objects exhibiting many forms of variability, but the numbers of known variable stars and recognition of variability phenomena are biased toward the most easily detected and studied. Specifically, individual stars or classes of stars that are rare, exhibit only low-amplitude variations (~0.01 mag or less), have relatively long or very short timescales of variation, or vary infrequently may go unrecognized if the photometric precision and time sampling is insufficient or if the number of stars observed is small.

Wide-field surveys employing time-series CCD photometry can fill in the gaps in our understanding of a variety of variable stars and related phenomena. Time-series photometry to find microlensing events has provided a large database of variable stars (e.g., MACHO, Alcock et al. 1995 and subsequent papers; Optical Gravitational Lensing Experiment-2, Żebruń et al. 2001; EROS-2, Bauer et al. 1999; Microlensing Observations in Astrophysics, Hearnshaw et al. 2000), as have optical all-sky surveys (e.g., All-Sky Automated Survey, Pojmański 2000; Robotic Optical Transient Search Experiment, Akerlof et al. 2000; *Hipparcos*, Eyer & Grenon 1997), deep imaging surveys (e.g., the Faint Sky Variability Survey; P. J. Groot et al. 2002, in preparation), and current or future searches for extrasolar planet transits both from the ground (e.g., Planets in Stellar Clusters Extensive Search, Mochejska et al. 2002; Vulcan, Borucki et al. 2001; Stellar Astrophysics and Research on Exoplanets, Brown & Charbonneau 2000, Street et al. 2000; Extrasolar Planet Occultation Research, Mallen-Ornelas et al. 2001) and in space (e.g., the *Hubble Space Telescope*, Albrow et al. 2001; *COROT*, Roun et al. 1999; *Kepler*, Koch et al. 1998). Issues addressed by such surveys include the fraction of stars in each spectral class that are variable (Eyer & Grenon 1997), types of variable stars and their population in the Milky Way and nearby galaxies (e.g., papers by Alcock et al.; Żebruń et al. 2001), and the causes and characteristics of low-amplitude photometric variations (<1%) in stars. Surveys can also be used to discover rare and unrecognized types of variable objects and to determine those individual stars and types of stars useful as photometric or astrometric standards by virtue of their non-variability in magnitude or photocenters (e.g., Eyer & Grenon 1997; Adelman 2001).

Here we present a statistical study of photometric V variability in a wide-field survey of field stars observed over 5 nights. This study follows up observations, data reduction,

[1] Visiting Astronomer, Kitt Peak National Observatory.

and analysis presented in Everett & Howell (2001). In § 2 we briefly review the observations and data reduction. In § 3 we assess the fraction of variable field stars as a function of color and magnitude and then present results for a few examples of specific variable stars. We discuss the contribution to the variable star population by both pulsating and eclipsing variables. In § 4 we discuss implications of stellar variability for future projects including searches for extrasolar planet transits and space astrometry missions.

TABLE 1
SURVEY FIELDS

Field	$\alpha_{J2000.0}$	$\delta_{J2000.0}$	l (deg)	b (deg)	Number of Observations
1	06 06 00	+45 40 00	167	+12	200
2	14 09 30	+53 20 00	99	+60	250

NOTE.—Units of right ascension are hours, minutes, and seconds, and units of declination are degrees, arcminutes, and arcseconds.

2. OBSERVATIONS AND DATA REDUCTION

On 2000 March 16–20 UT we observed a time series of images in *V* and one or two images each in *UBRI* toward two $59' \times 59'$ fields using the NOAO Mosaic Camera at the Kitt Peak 0.9 m telescope. Table 1 gives the centers and number of observations taken toward each field. The time series consist of 180 s exposures toward each field on 5 consecutive nights, giving a time sampling of 5.7 minutes and 4–5 hr of coverage per night on each field. The effective magnitude range is $V = 13.8$–19.5 for the stars with complete light curves.

The images are reduced by subtracting an overscan bias followed by a residual two-dimensional bias pattern and then are flat-fielded using dome flats. The stars in each field are located using IRAF scripts (Tody 1986) employing DAOfind. After identifying the same set of stars in each *V* exposure, we use IRAF's PHOT task to perform aperture photometry on each star through five differently sized apertures. The instrumental magnitudes for each star in each exposure are corrected for changes in seeing and atmospheric transparency using differential photometry performed by our FORTRAN codes. The uncertainty for each magnitude is also calculated including all relevant sources of error. Our differential photometry code uses an ensemble of nonvariable comparison stars found near each star in the field. Finally, the magnitudes are placed on a standard scale using observations taken toward a standard field of Landolt (1992). The light curves produced consist of up to 200 and 250 data points for our two fields. The *UBRI* magnitudes for each star are found and placed on a standard scale in the same way as for the *V* magnitudes. A more thorough discussion of the observations and reduction procedures is given by Everett & Howell (2001, hereafter EH). Reduced light-curve data from this survey are available upon request.

We match stars in the fields with positions from the USNO-A V2.0 Catalog (Monet et al. 1998) to obtain a plate solution for each CCD. The positions found for our objects are accurate to within $\sim 2''$.

3. RESULTS

3.1. Cosmic-Ray Rejection

Before we analyze the light curves, we must reject those magnitudes in error because of cosmic-ray hits in the photometry aperture. The IRAF scripts that perform the initial photometry normally do not record cosmic-ray events as errors. Cosmic-ray contamination manifests itself as light-curve data points with anomalously high fluxes. To reject these data from otherwise nonvariable light curves, we flag with an error any data point that is brighter than the mean magnitude by at least 3.5 times the light curve's standard deviation. The only light curves that are not subject to this procedure are those in which four or more deviant data points are found (which would most likely occur in the light curve of a variable object) or in cases in which two or more of the discrepant data points are consecutive in time.

3.2. Photometric Quality

We have light curves for ~12,000 stars in the two fields. In the case of the brightest stars observed ($V = 13.8$), our average per-exposure photometric precision is 0.002 mag. The precision worsens for fainter stars to ~0.2 mag at $V = 19.5$, at which point stars become undetectable in those exposures taken during relatively poor seeing or transparency. In total, there are approximately 2000 light curves brighter than $V = 16.5$, the magnitude corresponding to a photometric precision of 0.01 mag.

By binning and averaging light-curve data points for each night, we can obtain light curves with a higher photometric precision per data point, at the trade-off of sampling only once per night. In this case, photometric precisions range from 0.00019 to 0.013 mag over the $V = 13.8$–19.5 magnitude range. This precision determines our ability to detect photometric variations on a night-to-night timescale. A complete analysis of the precision for our light curves is given by EH.

The photometric accuracy in our *V*-band light curves and *UBVRI* color photometry (as opposed to the internal point-to-point precision of the light curves) is more difficult to determine and quantify. We have not sought a detailed calibration between our stellar colors and those of a standard system since our primary interest is detecting variability. Our stellar colors agree within 0.15 mag of the main-sequence loci found on other broadband photometric systems (see EH). We use the *UBVRI* photometry as a means to estimate the magnitude and spectral type of each star in the field. Our intentions are to obtain detailed follow-up observations, especially spectra, to study and classify the most interesting stars.

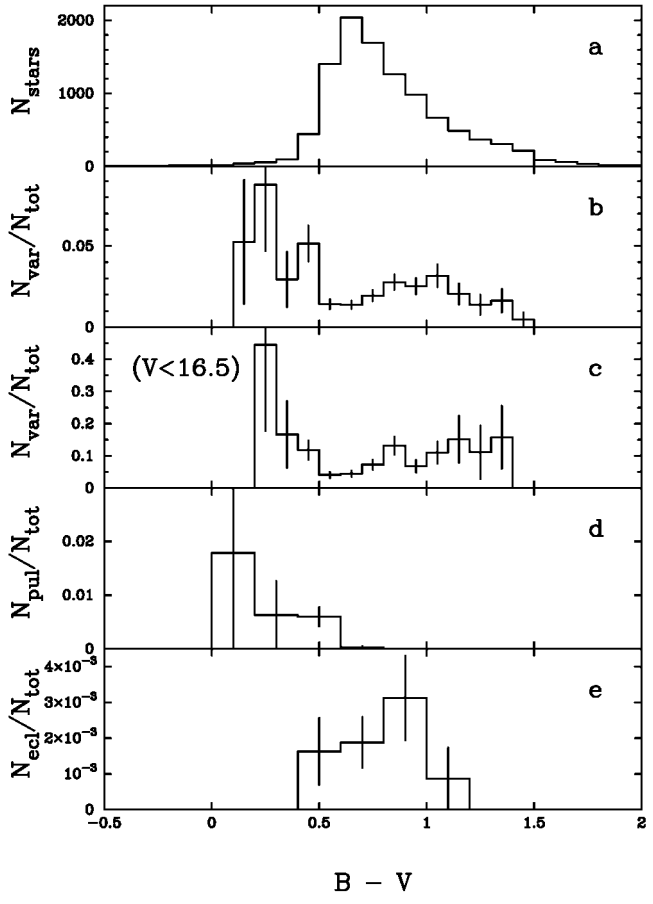

FIG. 1.—(*a*) Distribution in the number of surveyed stars detectable in both *B* and *V* as a function of $B-V$. There are 10,334 stars shown here. (*b*) Fraction of stars whose light curves are found to be variable as a function of $B-V$ for stars at all values of *V*. (*c*) Fraction of stars whose light curves are found to be variable as a function of $B-V$ for stars in the magnitude range $13.8 < V < 16.5$. (*d*) Fraction of all stars classified as pulsating variables as a function of $B-V$. (*e*) Fraction of all stars classified as eclipsing variables as a function of $B-V$.

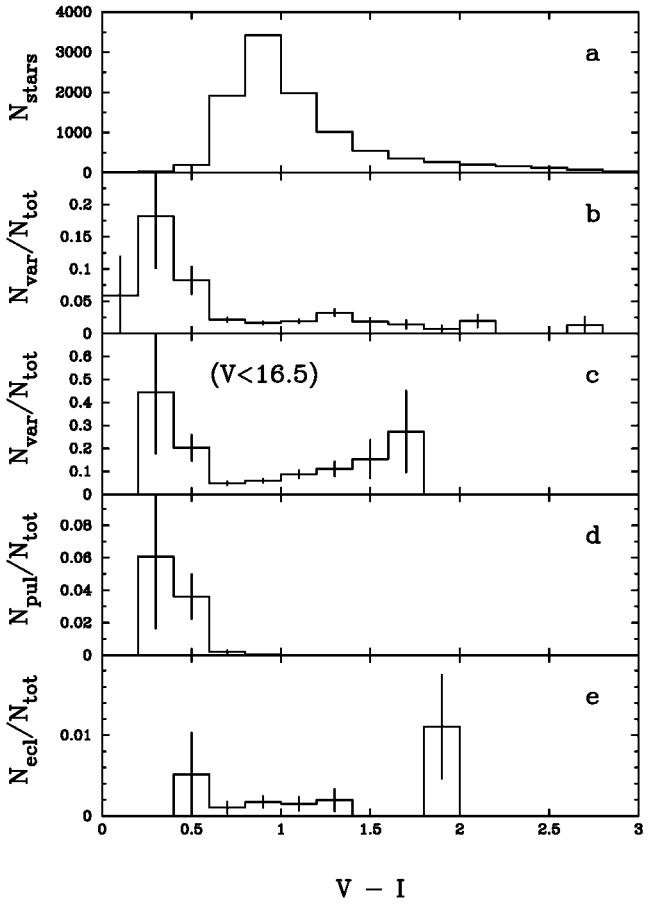

FIG. 2.—Same as Fig. 1 but for surveyed stars detectable in both *V* and *I* as a function of $V-I$. There are 10,398 stars shown here.

3.3. Light-Curve Testing

Variable objects are detected and categorized by calculating statistics or visually inspecting each light curve. These statistical tests include the following:

1. χ^2 for constant fit test: A weighted mean magnitude is calculated as a fit for the light curve, and the χ^2 value for this fit is found. The probability that random fluctuations (noise) in a nonvariable light curve would have exceeded this value of χ^2 is calculated and taken as a measurement for the likelihood that the light curve is variable.

2. Test for periodic variability: We check for periodicity in light curves using the "Lomb method" algorithm described by Press et al. (1992), which can accommodate light curves that are unevenly sampled in time. We search for periods between 12 minutes and 4.2 days (in the case of stars having complete light curves). This is the range allowed by our time sampling in the present data set.

3.4. Variability versus Color and Magnitude

In Figure 1*a* we plot the number of stars in our two fields versus their $B-V$ colors. The histogram shows that 71% of the stars detectable in both *B* and *V* fall in the range $B-V = 0.5$–1.0, colors that correspond to main-sequence spectral types F8–K3 (Cox 2000). We plot the corresponding color distribution of $V-I$ in Figure 2*a*. Again, the color distribution peaks in a range that corresponds to solar-like spectral types. We combined the stellar colors of our two fields together, noting that there is little detectable difference between the color distributions in these fields although their locations and stellar densities are very different (our low Galactic latitude field contains 6 times as many stars as the high Galactic latitude field).

This survey is dominated by solar-type stars, as previously discussed by EH. However, some giants are expected in these fields. The Galaxy models of Bahcall & Soneira (1980) predict that in both fields combined, 5% of all stars detected in *V* and 14% of the bright stars ($13.8 < V < 16.5$) will be giants.

Luminosity classes are difficult to differentiate for stars over most of our observed temperature sequence using only broadband colors. In § 3.8, we discuss the identification of individual giants and their contribution to stellar variability in this survey.

To examine how variability depends on spectral type, we determine the fraction of stars that are variable as a function of $B-V$ and $V-I$. The χ^2 for a constant-fit test (see § 3.3) is best suited to detect a wide range of variability types. It is used to classify stars as either variable or nonvariable (e.g., to construct Figs. 1 and 2). A conservative threshold on the probability of variability is adopted based on visual inspection of a large number of the light curves. Complete light curves (with the star detected in each exposure) all have reduced χ^2 values exceeding 1.6. Additionally, the light curve of each star statistically measured to be variable, and if necessary an image, is inspected by eye to ensure that no problematic data (e.g., stars subject to the scattered light of bright stars in the field or obvious galaxies located by DAOfind) are included in the sample. There are a total of 222 variable stars found by these methods, and 214 and 219 of these have $V-I$ and $B-V$ color measurements, respectively. The positions, magnitudes, and colors of all 222 variables are listed in Table 2. The identification numbers are composed of three digits representing a field number (1 or 2), a CCD number (CCDs 1–8 as designated by the Mosaic Camera software), and a number for each star detected on that CCD.

Figure 1*b* shows the fraction of all stars found to be variable as a function of $B-V$ (the "variable fraction"). The variable fraction ranges from ~1% to at least 5% over the color range $B-V = 0$–1.5. The uncertainties for the fractions plotted in Figure 1 (as well as in Figs. 2 and 4) were calculated assuming that the total number of stars in each bin, N, and the number of variable stars in each bin, N_v, were uncertain by $\sqrt{N}$ and $\sqrt{N_v}$, respectively, and that these could be propagated as independent, normal errors to find an uncertainty in the ratio N_v/N of $N^{-1}[N_v(1 + N_v/N)]^{1/2}$. A few stars with $B-V$ colors lie outside the range plotted in Figure 1; 49 stars have colors bluer than $B-V = 0.1$, and 218 have colors redder than $B-V = 1.5$. None of these stars appears to be variable, but because the variable fraction is only a few percent at other $B-V$ values, there is no significant change detected in the variable fraction at these colors.

Figure 1*b* shows the highest fraction of variability occurring in stars in the color range $B-V = 0.1$–0.5 where approximately 5% of the stars exhibit variability. The fraction of variable stars drops significantly with redder colors, and stars in the color range $0.5 < B-V < 0.7$ (like the Sun) show a low variable fraction of ~1.4%. There is a secondary peak in the variable fraction distribution around $B-V = 1.0$, where it reaches 3%.

In Figure 2*b* we plot the fraction of all stars found to be variable versus their $V-I$ colors. As with the variable fraction versus $B-V$, the variable fraction is maximum in the relatively blue color range $V-I = 0$–0.6. The variable fraction drops rather sharply at colors redder than this before increasing to a mild secondary peak at $V-I \simeq 1.3$.

In Figures 1*b* and 2*b* the decrease in variability fraction with redder colors starting at $B-V \simeq 1$ and $V-I \simeq 1.3$ is most likely due to the relative faintness of the reddest stars in the field. We are less sensitive to detecting variations in the reddest stars because on average their light curves are noisier than those of the blue stars.

Figures 1*c* and 2*c* show the fraction of all stars with $V < 16.5$ found to be variable versus $B-V$ and $V-I$, respectively. We found that 148 of the 1977 stars brighter than $V = 16.5$ are variable (i.e., 7.5%). Stars brighter than $V = 16.5$ have light curves whose mean uncertainty per data point is $\sigma \simeq 0.01$ mag or better. By restricting the magnitude range to $V = 13.8$–16.5, we eliminate the noisy light curves of faint stars for which we are insensitive to detecting low-level variability. This reduces any effects on the variable fraction that arise because of correlations between color and magnitude as seen in both Figures 1*b* and 2*b*. When comparing Figures 1*c* and 2*c* to Figures 1*b* and 2*b*, we find that the fraction of stars that are variable increases by a factor of 3 once the sample is restricted to the bright magnitudes (i.e., high photometric precisions). The shapes of the distributions change slightly as well, although with the large uncertainties in some color bins, this change is marginal. The peak in the variable fraction among the bluest stars is still apparent in Figures 1*c* and 2*c*. However, the decrease in variable fraction in the reddest stars is no longer seen in either $B-V$ or $V-I$. In fact, the reddest bins appear to contain a relatively high variable fraction.

Eyer & Grenon (1997) calculated the "mean intrinsic scatter" for light curves of stars in the *Hipparcos* Catalogue as a function of temperature and luminosity class. They define the intrinsic scatter of a light curve, $\sigma_{\rm int}$, in the following manner:

$$\sigma_{\rm int}^2 = \sigma_{\rm data}^2 - \epsilon_{\rm int}^2.$$

Here $\sigma_{\rm data}^2$ is the variance in the light-curve points for all stars observed (variable and nonvariable) and $\epsilon_{\rm int}^2$ is the expected variance in the same data due to noise. The contribution to the intrinsic scatter due to nonvariable stars is zero if a mean is taken of many such stars.

In order to compare our results with those of Eyer & Grenon (1997), particularly for the main-sequence stars that dominate our numbers, we have calculated the mean intrinsic scatter, $\langle\sigma_{\rm int}\rangle$, for our data as a function of $V-I$. We include only stars with $V < 19$ to omit those stars near the detection limit that are observed in relatively few exposures. We plot the results in Figure 3. The absolute level of $\langle\sigma_{\rm int}\rangle$ reflects the influence of the many nonvariables used in its calculation and is less important than the shape, which depends on the numbers and amplitudes of variables at each color. Figure 3 shows a relatively high $\langle\sigma_{\rm int}\rangle$ around $V-I = 0.5$ and low values immediately on either side of this color. The value of $\langle\sigma_{\rm int}\rangle$ increases

TABLE 2
VARIABLE STARS

Identification Number	$\alpha_{J2000.0}$	$\delta_{J2000.0}$	V	$U-B$	$B-V$	$V-R$	$B-I$	$V-I$	Class[a]
1-4-0020	06 03 15.1	+45 23 22	19.7	0.1	1.0	0.6	2.6	1.5	U
1-4-0018	06 03 15.2	+45 14 48	16.2	0.1	0.7	0.4	1.6	0.9	U
1-1-0033	06 03 16.2	+46 07 55	17.0	0.0	0.7	0.5	1.6	1.0	EA*
1-1-0036	06 03 16.6	+46 08 12	16.0	0.0	0.5	0.3	1.1	0.7	U
1-2-0038	06 03 17.0	+45 54 20	16.2	0.1	0.7	0.4	1.7	1.0	U
1-1-0041	06 03 17.4	+46 02 28	14.8	0.1	0.7	0.4	1.7	0.9	U
1-1-0054	06 03 18.4	+46 08 34	19.0	0.3	1.4	0.9	3.0	1.6	U
1-2-0049	06 03 18.8	+45 45 01	15.2	1.0	1.0	0.6	2.3	1.2	U
1-1-0059	06 03 19.7	+46 04 42	16.9	0.9	1.0	0.6	2.4	1.4	U
1-4-0076	06 03 21.2	+45 18 58	17.9	0.1	1.0	0.5	2.1	1.1	U
1-4-0082	06 03 21.8	+45 22 25	15.2	0.4	0.9	0.5	2.0	1.1	U*
1-1-0071	06 03 22.5	+46 06 60	17.6	0.6	1.0	0.7	2.4	1.4	EA
1-4-0126	06 03 25.9	+45 20 53	17.0	0.2	0.8	0.4	1.7	0.9	U
1-4-0127	06 03 26.2	+45 11 07	16.7	0.2	0.7	0.4	1.7	0.9	U
1-1-0094	06 03 26.4	+45 57 40	18.3	0.2	0.9	0.5	2.0	1.1	U
1-4-0154	06 03 28.9	+45 19 47	17.7	0.3	0.9	0.4	1.9	1.0	U
1-1-0121	06 03 29.0	+46 09 08	16.0	0.0	0.6	0.3	1.2	0.7	U
1-3-0242	06 03 33.6	+45 26 32	15.2	0.0	0.5	0.3	1.2	0.7	U
1-3-0244	06 03 34.2	+45 37 31	20.3	0.8	−1.1	1.4	0.3	1.4	U
1-1-0167	06 03 34.6	+46 07 19	15.1	0.0	0.7	0.4	1.5	0.8	U
1-2-0188	06 03 35.8	+45 49 03	19.4	−0.5	0.9	0.4	1.9	1.0	U
1-4-0247	06 03 38.7	+45 24 00	15.1	0.0	0.6	0.4	1.5	0.8	U
1-4-0283	06 03 43.2	+45 20 47	15.1	0.7	1.1	0.6	2.4	1.3	U
1-1-0234	06 03 44.0	+46 03 55	15.7	0.5	0.9	0.5	2.0	1.1	U
1-2-0263	06 03 44.0	+45 41 40	13.9	1.2	1.2	0.7	…	…	U
1-2-0315	06 03 50.5	+45 51 55	17.1	0.0	0.7	0.5	1.7	1.0	EW
1-4-0369	06 03 51.2	+45 20 02	16.8	1.2	1.4	0.9	3.6	2.2	U
1-1-0289	06 03 52.2	+45 57 09	17.7	…	…	…	0.3	…	U
1-3-0402	06 03 52.5	+45 32 02	16.4	0.7	1.0	0.6	2.1	1.2	U
1-1-0298	06 03 52.9	+45 56 11	15.5	0.0	0.5	0.3	1.2	0.7	SX Phe/δ Scuti*
1-3-0405	06 03 52.9	+45 33 27	14.7	0.4	0.8	0.5	1.7	0.9	U
1-3-0414	06 03 53.2	+45 29 34	13.8	0.9	1.0	0.6	…	…	U
1-4-0400	06 03 53.6	+45 13 38	15.5	0.0	0.4	0.3	1.0	0.5	U
1-4-0415	06 03 55.0	+45 24 00	14.5	0.1	0.7	0.4	1.5	0.8	U
1-2-0413	06 03 59.9	+45 45 41	17.5	0.5	0.8	0.5	1.9	1.0	U
1-4-0468	06 04 00.1	+45 24 25	14.2	0.2	0.7	0.4	1.5	0.8	U
1-2-0419	06 04 00.6	+45 49 12	15.0	0.7	1.0	0.6	2.2	1.2	U
1-1-0373	06 04 01.4	+46 00 04	16.5	0.6	1.0	0.5	2.2	1.2	U
1-2-0442	06 04 02.1	+45 47 28	14.6	0.4	0.8	0.4	1.7	0.9	U*
1-2-0458	06 04 04.2	+45 54 30	15.4	1.2	1.2	0.6	2.5	1.3	U
1-3-0518	06 04 05.2	+45 37 48	15.3	0.3	0.8	0.5	1.8	1.0	U
1-4-0528	06 04 07.1	+45 11 12	15.6	0.0	0.5	0.3	1.1	0.6	U
1-4-0566	06 04 09.8	+45 23 01	15.5	0.2	0.8	0.5	1.7	0.9	U
1-4-0567	06 04 09.9	+45 24 09	16.3	0.5	0.9	0.5	1.9	1.1	U
1-4-0611	06 04 14.2	+45 14 29	17.0	0.6	0.9	0.6	2.1	1.2	U
1-3-0612	06 04 15.6	+45 29 26	15.7	0.1	0.3	0.2	0.6	0.3	U
1-4-0639	06 04 17.1	+45 12 43	15.2	0.0	0.6	0.4	1.5	0.8	U
1-4-0641	06 04 17.1	+45 16 47	14.5	1.2	1.3	0.8	…	…	U
1-4-0649	06 04 17.6	+45 12 03	19.3	…	0.9	0.8	2.7	1.8	U
1-3-0647	06 04 18.5	+45 38 29	15.0	0.6	0.8	0.5	1.8	1.0	U
1-4-0663	06 04 18.9	+45 11 16	15.6	0.1	0.6	0.4	1.4	0.8	U
1-2-0622	06 04 21.9	+45 53 54	15.3	0.4	0.8	0.5	1.8	1.0	U
1-4-0697	06 04 22.1	+45 22 08	18.4	1.1	1.1	0.6	2.4	1.3	U
1-1-0568	06 04 23.3	+45 56 24	15.0	0.2	0.8	0.5	1.9	1.1	U*
1-4-0741	06 04 25.4	+45 15 23	17.1	1.1	1.5	0.9	4.1	2.7	U
1-4-0751	06 04 26.7	+45 23 55	17.4	1.0	1.2	0.9	3.3	2.0	U
1-1-0617	06 04 28.2	+46 00 37	17.1	0.7	1.0	0.6	2.3	1.3	U
1-1-0634	06 04 30.2	+46 06 54	16.9	0.7	1.0	0.6	2.3	1.3	U
1-1-0637	06 04 30.4	+46 05 52	15.7	1.4	1.3	0.8	3.1	1.8	U
1-1-0645	06 04 31.6	+46 05 43	14.4	0.2	0.5	0.3	1.0	0.6	SX Phe/δ Scuti*

TABLE 2—*Continued*

Identification Number	$\alpha_{J2000.0}$	$\delta_{J2000.0}$	V	$U-B$	$B-V$	$V-R$	$B-I$	$V-I$	Class[a]
1-3-0793	06 04 32.3	+45 27 18	14.4	0.1	0.6	0.3	1.4	0.7	U
1-1-0680	06 04 35.0	+45 56 58	14.6	0.5	0.9	0.5	2.0	1.1	U
1-1-0711	06 04 38.2	+46 07 03	13.9	0.1	0.5	0.3	1.2	0.7	SX Phe/δ Scuti*
1-3-0876	06 04 39.4	+45 38 19	15.9	0.0	0.5	0.3	1.1	0.6	U
1-2-0796	06 04 42.1	+45 42 57	14.0	0.1	0.6	0.4	1.4	0.8	U
1-2-0798	06 04 42.5	+45 45 11	19.9	0.1	0.8	1.2	2.8	2.0	EW
1-3-0975	06 04 48.2	+45 33 29	13.8	0.1	0.6	0.4	1.3	0.7	U
1-1-0838	06 04 50.8	+46 00 02	14.9	0.0	0.6	0.4	1.4	0.8	SX Phe/δ Scuti*
1-4-1009	06 04 54.9	+45 11 31	14.1	1.0	1.1	0.6	2.3	1.2	U
1-4-1033	06 04 56.6	+45 20 32	15.7	0.7	0.9	0.6	1.9	1.1	U
1-4-1044	06 04 57.4	+45 12 17	14.8	0.0	0.6	0.5	1.4	0.9	EW*
1-2-0950	06 04 58.9	+45 51 33	15.9	0.0	0.5	0.3	1.2	0.7	EW*
1-3-1103	06 04 59.8	+45 26 17	14.3	0.2	0.7	0.4	1.4	0.8	U
1-4-1085	06 05 01.3	+45 13 18	14.1	0.1	0.6	0.4	1.4	0.7	U
1-1-0926	06 05 02.7	+46 01 59	18.6	0.9	0.5	0.5	1.5	1.0	U
1-1-0949	06 05 05.4	+45 56 04	14.7	0.5	0.8	0.5	1.8	1.0	U*
1-4-1128	06 05 06.2	+45 19 49	15.8	0.1	0.6	0.4	1.4	0.8	EA*
1-2-1046	06 05 07.8	+45 44 53	15.5	1.0	1.0	0.6	2.3	1.2	U
1-4-1145	06 05 08.2	+45 16 51	17.2	0.5	0.9	0.6	2.1	1.2	U*
1-2-1070	06 05 09.6	+45 43 27	14.9	0.1	0.2	0.1	0.4	0.2	U
1-3-1194	06 05 10.4	+45 36 13	15.2	0.1	0.4	0.3	1.0	0.6	SX Phe/δ Scuti*
1-2-1099	06 05 12.6	+45 43 16	14.6	0.2	0.7	0.4	1.6	0.9	U
1-4-1197	06 05 13.2	+45 12 51	17.2	0.1	0.7	0.4	1.6	0.9	EW
1-3-1228	06 05 13.9	+45 27 09	14.1	0.6	0.8	0.5	1.8	1.0	U
1-3-1223	06 05 14.0	+45 35 20	16.7	0.7	1.0	0.7	2.3	1.3	EW*
1-4-1221	06 05 16.5	+45 19 41	14.6	0.2	0.7	0.4	1.5	0.8	U
1-3-1285	06 05 19.0	+45 27 42	18.4	0.4	0.7	0.3	1.5	0.8	U
1-1-1091	06 05 23.6	+46 07 28	18.8	0.6	0.9	1.2	2.9	1.9	EW
1-4-1292	06 05 24.9	+45 10 41	16.0	1.1	1.0	0.7	2.3	1.3	U
1-4-1304	06 05 26.0	+45 20 30	15.0	0.1	0.5	0.4	1.1	0.7	U
1-1-1108	06 05 26.1	+46 04 58	18.9	0.9	0.3	0.4	1.0	0.8	U
1-4-1316	06 05 27.5	+45 14 39	16.2	0.1	0.4	0.3	0.9	0.5	U*
1-2-1255	06 05 27.7	+45 41 21	14.3	0.1	0.6	0.4	1.4	0.8	U
1-3-1396	06 05 31.8	+45 32 13	15.2	0.8	0.9	0.6	2.0	1.1	U
1-3-1439	06 05 35.7	+45 33 15	14.3	1.8	1.4	0.8	…	…	U
1-2-1338	06 05 36.9	+45 41 08	14.6	0.1	0.5	0.3	1.1	0.6	U
1-3-1460	06 05 38.4	+45 34 22	19.2	1.0	1.1	0.8	3.2	2.1	U*
1-3-1466	06 05 38.8	+45 26 22	14.4	1.4	1.2	0.7	2.6	1.4	U*
1-1-1222	06 05 40.6	+46 07 29	17.4	0.9	1.2	0.8	2.8	1.6	U
1-2-1389	06 05 41.3	+45 44 22	16.1	0.8	0.9	0.6	2.1	1.1	U
1-2-1395	06 05 42.6	+45 53 52	15.4	0.9	1.0	0.6	2.3	1.3	U
1-3-1498	06 05 43.5	+45 37 27	16.9	0.2	0.8	0.5	1.8	1.0	U
1-4-1499	06 05 48.0	+45 22 42	14.8	0.3	0.7	0.5	1.6	0.9	U
1-1-1299	06 05 50.8	+45 55 12	14.1	0.1	0.4	0.2	1.0	0.5	SX Phe/δ Scuti*
1-1-1302	06 05 51.9	+46 08 26	14.3	1.2	1.1	0.7	2.6	1.5	U
1-1-1315	06 05 52.7	+45 55 53	16.4	0.2	0.7	0.5	1.7	1.0	U
1-8-0016	06 06 01.3	+45 20 15	15.4	1.3	1.2	0.7	2.6	1.4	U
1-8-0022	06 06 02.5	+45 12 34	14.6	0.9	0.9	0.6	2.1	1.2	U
1-8-0055	06 06 06.5	+45 20 59	14.7	0.1	0.4	0.3	1.0	0.6	U
1-7-0067	06 06 06.6	+45 32 33	15.3	0.2	0.3	0.2	0.6	0.3	U
1-7-0089	06 06 08.2	+45 33 02	18.4	0.9	1.2	0.8	3.0	1.8	EW*
1-5-0091	06 06 09.7	+46 07 32	18.4	0.0	0.7	0.4	1.8	1.0	U
1-8-0084	06 06 10.0	+45 18 51	14.6	0.4	0.7	0.5	1.7	0.9	U
1-5-0122	06 06 13.3	+46 07 18	16.3	…	…	…	…	…	U
1-7-0149	06 06 13.8	+45 27 49	18.7	0.0	0.7	0.1	1.1	0.4	EW
1-6-0118	06 06 13.9	+45 50 04	15.6	0.2	0.7	0.4	1.6	0.9	U
1-7-0239	06 06 24.6	+45 36 48	19.6	0.6	0.7	0.5	1.6	0.9	U
1-6-0237	06 06 27.2	+45 46 57	15.3	0.5	0.8	0.5	1.9	1.0	EA*
1-5-0276	06 06 28.0	+46 00 34	19.0	0.7	0.7	0.8	2.2	1.4	U
1-8-0243	06 06 29.0	+45 21 24	15.9	0.2	0.7	0.5	1.8	1.0	U

TABLE 2—*Continued*

Identification Number	$\alpha_{J2000.0}$	$\delta_{J2000.0}$	V	$U-B$	$B-V$	$V-R$	$B-I$	$V-I$	Class[a]
1-8-0262	06 06 31.3	+45 14 00	17.4	0.1	0.6	0.4	1.4	0.8	U
1-6-0301	06 06 33.0	+45 47 49	14.7	0.1	0.6	0.4	1.4	0.7	U
1-7-0327	06 06 35.8	+45 38 21	14.1	0.1	0.5	0.4	1.2	0.7	U
1-6-0355	06 06 38.9	+45 53 24	15.5	0.4	0.8	0.5	1.8	1.0	U
1-7-0365	06 06 39.4	+45 38 20	15.9	0.0	0.5	0.4	1.2	0.7	U
1-8-0323	06 06 40.8	+45 21 02	15.5	0.1	0.4	0.3	1.0	0.6	SX Phe/δ Scuti*
1-5-0416	06 06 41.6	+46 02 59	15.0	0.2	0.7	0.4	1.6	0.9	U
1-6-0388	06 06 41.8	+45 47 55	15.9	0.0	0.6	0.4	1.4	0.8	U
1-7-0391	06 06 41.9	+45 38 10	14.7	0.1	0.4	0.3	1.0	0.6	U
1-5-0421	06 06 42.3	+45 57 07	14.3	0.1	0.5	0.3	1.2	0.6	U
1-6-0395	06 06 42.3	+45 50 42	16.3	0.1	0.6	0.4	1.4	0.8	U*
1-8-0338	06 06 42.8	+45 14 55	18.8	0.0	0.9	0.5	1.9	1.0	EW
1-6-0424	06 06 45.1	+45 46 57	16.3	0.0	0.5	0.4	1.3	0.8	U
1-5-0466	06 06 47.8	+46 04 18	18.1	0.5	0.8	0.6	2.0	1.1	U
1-8-0401	06 06 49.3	+45 14 12	15.7	1.2	1.0	0.7	2.4	1.4	U
1-8-0402	06 06 49.8	+45 23 25	16.1	0.7	0.8	0.6	1.9	1.1	U
1-7-0503	06 06 51.8	+45 31 02	14.2	0.2	0.3	0.2	0.6	0.3	SX Phe/δ Scuti*
1-5-0502	06 06 51.9	+46 06 20	15.8	0.1	0.4	0.3	1.0	0.6	SX Phe/δ Scuti*
1-7-0508	06 06 52.7	+45 39 18	16.2	0.2	0.7	0.5	1.7	1.0	U
1-6-0507	06 06 53.9	+45 42 47	14.0	1.1	1.0	0.6	2.1	1.2	U
1-7-0527	06 06 54.4	+45 35 37	16.0	0.1	0.4	0.3	0.9	0.5	U
1-5-0543	06 06 56.0	+46 09 09	15.2	0.1	0.5	0.3	1.1	0.6	U
1-6-0565	06 06 60.0	+45 51 43	14.7	0.6	1.0	0.5	2.2	1.2	U
1-8-0518	06 07 02.8	+45 22 40	14.6	0.5	0.9	0.5	1.9	1.0	U
1-7-0661	06 07 06.4	+45 29 11	15.8	0.0	0.5	0.3	1.1	0.6	U
1-7-0668	06 07 07.2	+45 29 55	14.9	0.6	0.8	0.5	1.8	1.0	U
1-8-0567	06 07 08.2	+45 13 26	14.5	0.3	0.7	0.4	1.5	0.8	U
1-6-0658	06 07 09.6	+45 41 53	18.7	0.3	0.9	0.6	2.0	1.1	EW
1-6-0678	06 07 11.1	+45 47 49	14.4	0.8	1.0	0.6	2.2	1.2	U
1-5-0699	06 07 11.2	+45 57 30	15.8	0.7	0.9	0.5	1.9	1.0	U
1-7-0711	06 07 11.2	+45 28 02	14.9	0.0	0.5	0.4	1.2	0.7	U
1-6-0684	06 07 11.7	+45 48 53	16.6	0.0	0.5	0.3	1.2	0.7	U
1-5-0740	06 07 15.0	+46 00 05	16.4	1.1	1.1	0.7	2.7	1.6	U
1-5-0755	06 07 16.4	+46 09 01	15.5	0.1	0.6	0.3	1.3	0.7	U
1-6-0776	06 07 19.7	+45 43 24	16.0	0.4	0.7	0.5	1.6	0.9	U
1-7-0822	06 07 20.1	+45 25 58	15.6	0.1	0.6	0.5	1.6	1.0	EW
1-6-0814	06 07 24.1	+45 44 38	14.0	0.9	1.0	0.6	2.1	1.1	U
1-5-0832	06 07 24.8	+45 59 51	14.0	0.1	0.4	0.3	1.0	0.6	SX Phe/δ Scuti*
1-7-0872	06 07 25.2	+45 28 03	15.1	0.6	0.8	0.6	1.9	1.1	U
1-6-0839	06 07 26.3	+45 46 04	16.3	0.8	1.0	0.6	2.3	1.3	U
1-6-0844	06 07 27.1	+45 49 45	14.2	0.9	1.0	0.6	2.2	1.2	U
1-6-0868	06 07 29.8	+45 45 45	18.9	−0.2	0.7	0.4	1.4	0.7	U
1-8-0802	06 07 35.5	+45 14 49	14.1	0.1	0.6	0.4	1.4	0.8	U
1-8-0804	06 07 35.7	+45 16 00	14.9	0.1	0.5	0.4	1.1	0.7	U
1-6-0926	06 07 36.3	+45 48 48	16.0	0.5	0.8	0.5	1.7	1.0	U
1-7-0998	06 07 40.5	+45 32 59	15.1	0.2	0.4	0.3	1.0	0.6	SX Phe/δ Scuti*
1-5-1067	06 07 47.9	+45 54 54	14.1	1.2	1.0	0.7	…	…	U
1-5-1072	06 07 48.6	+46 07 11	14.4	0.6	0.8	0.5	1.7	0.9	U
1-5-1089	06 07 49.4	+45 55 25	17.2	0.8	0.9	0.7	2.4	1.4	U
1-7-1102	06 07 51.5	+45 30 28	16.4	0.1	0.4	0.3	0.9	0.5	U
1-7-1131	06 07 53.3	+45 25 51	17.6	0.6	1.0	0.6	2.4	1.4	U
1-6-1077	06 07 54.3	+45 44 50	15.5	0.5	0.8	0.5	1.7	0.9	U
1-5-1181	06 07 56.9	+46 02 58	16.7	0.0	0.5	0.3	1.2	0.7	U
1-6-1110	06 07 58.1	+45 50 30	14.6	0.2	0.6	0.4	1.4	0.8	U
1-5-1202	06 07 58.8	+46 07 05	14.1	0.2	0.7	0.4	1.5	0.8	SX Phe/δ Scuti*
1-5-1217	06 07 59.9	+46 03 32	17.4	0.1	0.6	0.5	1.5	0.9	EA*
1-8-1003	06 08 00.2	+45 10 46	17.1	0.2	0.2	0.2	0.5	0.3	U
1-5-1227	06 08 00.7	+46 03 26	17.5	0.5	0.8	0.5	1.9	1.1	U
1-7-1205	06 08 01.9	+45 39 21	15.1	0.7	0.8	0.6	1.9	1.1	U
1-5-1277	06 08 04.3	+46 08 00	18.8	0.1	0.6	0.4	1.5	0.9	U

TABLE 2—*Continued*

Identification Number	$\alpha_{J2000.0}$	$\delta_{J2000.0}$	V	$U-B$	$B-V$	$V-R$	$B-I$	$V-I$	Class[a]
1-5-1372	06 08 12.8	+46 02 14	15.3	0.7	0.9	0.5	1.9	1.1	U
1-7-1364	06 08 16.9	+45 33 03	15.7	1.0	0.9	0.6	2.1	1.2	U
1-8-1189	06 08 21.4	+45 18 30	16.3	…	…	…	…	…	U
1-8-1212	06 08 24.2	+45 15 15	15.9	0.5	0.7	0.5	1.7	1.0	U
1-6-1344	06 08 25.2	+45 53 42	15.7	0.7	0.8	0.5	1.9	1.0	U
1-6-1364	06 08 26.5	+45 44 34	16.2	0.7	0.8	0.5	1.9	1.0	U
1-7-1460	06 08 29.4	+45 39 12	14.4	0.8	0.8	0.5	1.8	1.0	U
1-8-1261	06 08 30.4	+45 11 18	13.8	0.1	0.5	0.3	1.2	0.7	U
1-8-1277	06 08 32.9	+45 13 41	14.5	0.3	0.6	0.4	1.5	0.8	U
1-8-1273	06 08 33.1	+45 18 25	18.8	0.8	0.5	0.7	1.6	1.1	U
1-8-1287	06 08 35.0	+45 20 36	17.0	0.8	1.0	0.6	2.4	1.4	U
1-6-1447	06 08 37.0	+45 42 34	14.4	0.9	0.9	0.6	2.0	1.1	U
1-8-1330	06 08 39.8	+45 13 58	19.4	2.7	1.1	0.8	2.5	1.5	U
1-8-1339	06 08 41.2	+45 13 57	15.5	0.7	0.7	0.4	1.5	0.9	U
1-8-1358	06 08 42.9	+45 11 01	19.1	0.5	0.5	0.4	1.4	0.9	U
2-2-0027	14 06 38.9	+53 21 42	17.7	0.7	1.0	0.6	2.3	1.3	U
2-2-0030	14 06 42.8	+53 24 42	18.4	−0.3	0.9	0.4	2.1	1.2	U
2-1-0076	14 07 53.1	+53 36 51	17.5	0.2	1.1	0.5	2.3	1.3	U
2-1-0083	14 07 58.9	+53 49 03	18.5	0.3	1.0	0.5	2.2	1.2	U
2-4-0188	14 08 19.5	+53 03 42	14.5	1.3	1.3	0.7	2.7	1.4	U*
2-3-0232	14 08 23.0	+53 18 47	17.4	0.1	0.7	0.4	1.6	0.8	U
2-3-0233	14 08 24.1	+53 06 52	16.3	0.5	1.0	0.6	2.4	1.3	U
2-4-0203	14 08 27.1	+53 04 08	16.8	0.3	1.0	0.6	2.3	1.3	U
2-3-0249	14 08 45.2	+53 16 44	17.1	0.9	1.0	0.7	2.5	1.5	U
2-4-0233	14 09 02.0	+52 56 15	16.5	0.4	0.7	0.4	1.6	0.9	U
2-2-0294	14 09 06.8	+53 27 49	17.2	0.5	1.2	0.6	2.7	1.5	U
2-3-0283	14 09 23.9	+53 11 13	18.0	0.2	1.1	0.6	2.4	1.3	U
2-7-0004	14 09 31.7	+53 10 13	14.1	1.1	1.0	0.7	2.3	1.2	U
2-5-0023	14 09 41.2	+53 48 07	17.7	0.6	1.2	0.5	2.5	1.3	U
2-6-0048	14 09 55.5	+53 24 20	14.3	0.2	0.7	0.4	1.6	0.9	U
2-5-0047	14 10 02.6	+53 48 21	17.6	−0.3	0.5	0.2	1.1	0.6	U
2-5-0048	14 10 03.6	+53 45 48	17.5	0.6	1.2	0.6	2.6	1.4	U
2-8-0069	14 10 47.9	+52 58 49	14.2	−0.1	0.6	0.4	1.4	0.8	U
2-7-0122	14 10 57.1	+53 13 36	17.3	−0.2	0.2	0.3	0.5	0.3	SX Phe/δ Scuti*
2-7-0123	14 10 57.2	+53 11 57	14.6	0.7	1.0	0.6	2.2	1.2	U
2-5-0121	14 10 58.5	+53 35 24	14.5	0.4	0.9	0.5	1.9	1.1	U
2-8-0080	14 11 05.7	+52 59 12	13.9	0.0	0.6	0.4	1.3	0.7	U
2-8-0083	14 11 07.3	+53 02 31	17.3	0.3	1.1	0.6	2.3	1.2	U
2-6-0264	14 11 31.5	+53 30 37	16.7	0.0	0.4	0.2	0.9	0.5	RR*ab* (CL Boo)
2-8-0141	14 12 20.2	+52 50 42	15.4	1.2	1.2	0.8	2.9	1.7	U
2-5-0220	14 12 25.5	+53 45 20	15.3	0.5	0.8	0.5	1.8	1.0	U
2-5-0224	14 12 29.3	+53 47 37	16.2	0.0	0.6	0.4	1.3	0.7	U

NOTE.—Units of right ascension are hours, minutes, and seconds, and units of declination are degrees, arcminutes, and arcseconds.

[a] Classification based on light curve; "U" indicates unclassified variables, and asterisks indicate stars with light curves presented in this paper (also listed in Table 3).

toward the red colors from its low value at $V-I = 0.7$. Some features in Figure 3 are similar to Eyer & Grenon's results for main-sequence *Hipparcos* stars. Eyer & Grenon (1997) identified low values for $\langle\sigma_{\rm int}\rangle$ (stable areas) on the main sequence on both sides of the instability strip. The instability strip, around F0 V, corresponds to the feature we find at $V-I = 0.5$. Eyer & Grenon (1997) found the most photometrically stable part of the main sequence between F2 and F9. We find the photometrically most stable color in a bin around $V-I = 0.7$, corresponding to the spectral types F4–G0 V, consistent with the results of Eyer & Grenon (1997).

Figure 4 shows the fraction of all stars that are variable versus their V magnitude. The trend seen with magnitude is expected because of the decreasing sensitivity to detecting variations as the light curves' noise increases with magnitude. What is more interesting is the fraction of stars with detectable variability at the bright end of our magnitude range (i.e., high photometric precisions). Approximately 17% of these stars are variable.

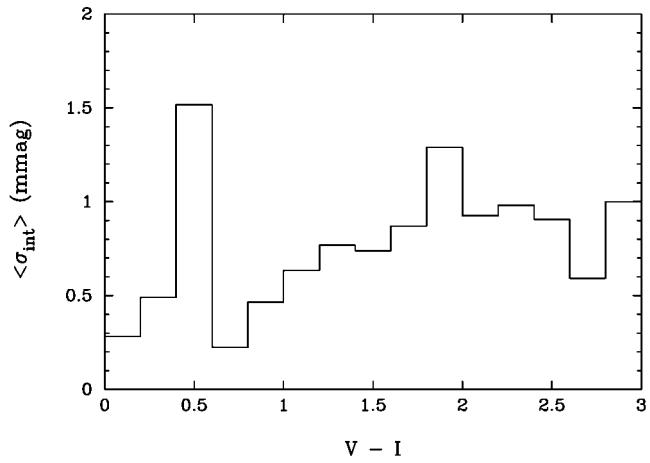

FIG. 3.—Mean intrinsic scatter, $\langle\sigma_{int}\rangle$, vs. $V-I$ for all stars (variables and nonvariables) with $V<19$. The mean intrinsic scatter reflects the amount of variability (both amplitude and percentage of variables) at each color. See the discussion in § 3.4.

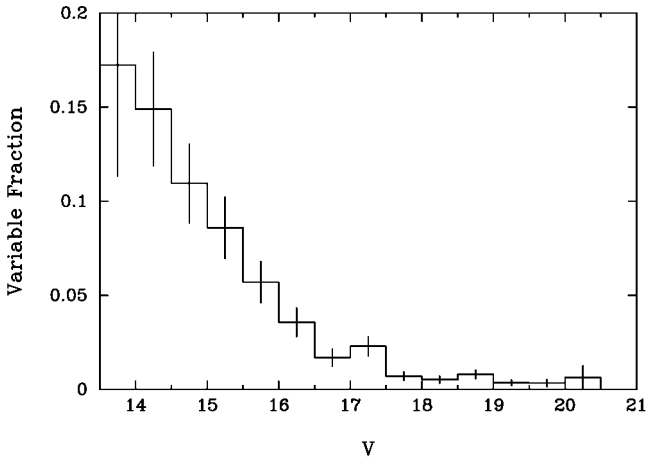

FIG. 4.—Fraction of all stars whose light curves are found to be variable vs. their V magnitude.

3.5. Pulsating Variables

A group of relatively blue variable stars in our fields are seen to have significant periodicity as found by the period-seeking routine described in § 3.3. Most have low-amplitude variations in V of 0.01–0.05 mag and $B-V$ colors of 0.4–0.55. When we inspect their light curves visually, we find that in most cases the variations cannot be explained by fitting a single periodic function but are likely to be described as a superposition of multiple periods. These stars are probably multi-period pulsating stars. The dominant periods seen in their light curves are one to a few hours, and this behavior combined with our particular time sampling makes these stars easy to recognize. Pulsating variables with long periods (days or more) would be more difficult to distinguish from spotted (rotating) variables, a population that is probably present in our data (see § 3.7). Pulsating variables with short periods ($\lesssim$10 minutes) are also difficult to detect given our time sampling of 6 minutes.

In Figures 5 and 6 we plot light curves for our best candidate

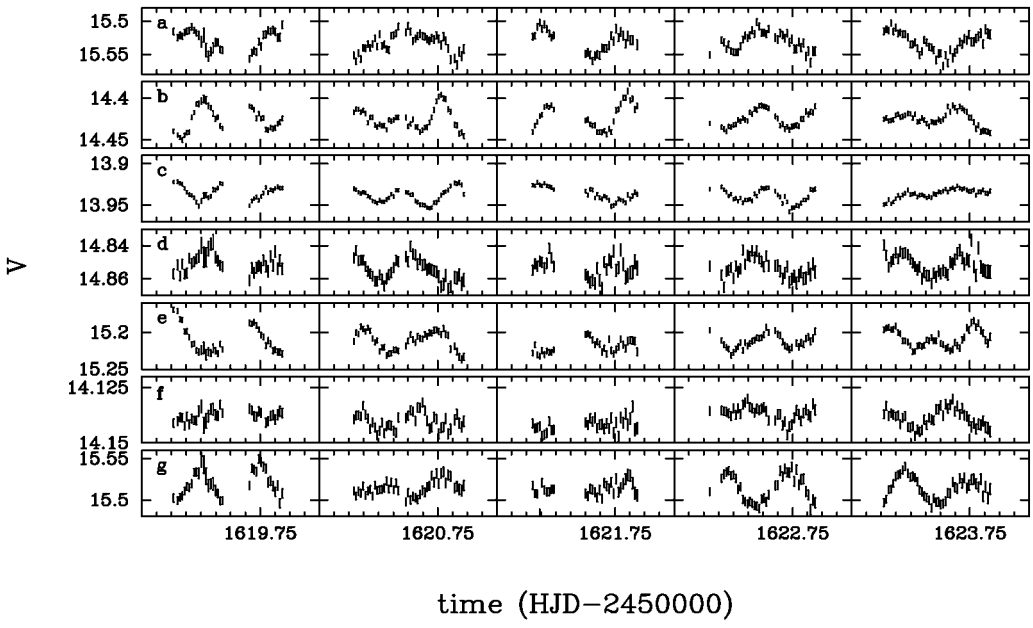

FIG. 5.—Sample light curves representing seven pulsating variables found in Field 1. Each star is observed on 5 consecutive nights. The 5 nights are plotted in five separate boxes. Tick marks on the time axis are in units of 0.6 hr. Information on each star represented here is given in Table 3.

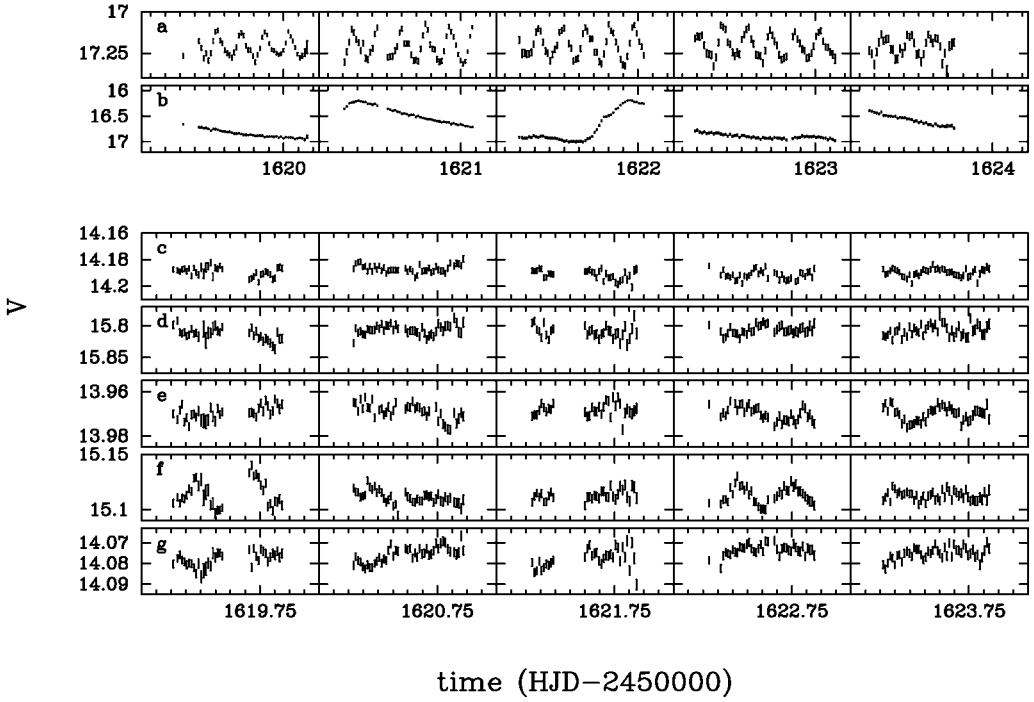

FIG. 6.—Sample light curves representing (*a*, *b*) two pulsating variables found in Field 2 and (*c*–*g*) five pulsating variables found in Field 1. See legend of Fig. 5 for details.

pulsating variable stars. Each night's observation is shown in a different panel. Table 3 includes identification numbers, a reference to the corresponding figure number and panel, and a preliminary classification for each star whose light curve is shown.

Most of the pulsating stars (13 of 14) represented in Figures 5 and 6 are classified as "SX Phe/δ Scuti" because their light curves are similar to those seen for these classes of variables (Feast 1996a; Poretti 2000; Breger 1980). Most appear to be low-amplitude members of these classes (Poretti 2000). The δ Scuti stars are Population I pulsating stars lying on or just off the main sequence, in the instability strip with spectral types A or F. The related SX Phoenicis class differs by being metal-poor Population II stars. The many types of pulsating stars and their locations on the H-R diagram are reviewed by Gautschy & Saio (1996) and these particular classes by Breger (2000). At $V = 14$–17, the luminosity of SX Phoenicis and δ Scuti stars ($M_V \simeq 2$–3) indicates a location in the Galactic halo. Thus, the stars we list as SX Phe/δ Scuti are probably SX Phe stars, but our classification is based on the light curves, which apparently do not distinguish between the two populations.

One of the stars that we identify as an SX Phe or δ Scuti variable has a significantly higher amplitude light curve and a relatively short period. Star 2-7-0122 has an amplitude of up to $\Delta V \sim 0.25$ and a relatively clear period of 58 minutes as seen in the light curve of Figure 6*a*. The slight modulations in the amplitude of this light curve hint of other periods.

One obvious example of an RR Lyrae star was found in our survey: star 2-6-0264 (see Fig. 6*b*). On the basis of its light curve that shows a relatively rapid rise toward maximum and slower fall-off in magnitude toward minimum, this star belongs to the RR Lyrae subclass RR*ab* (Feast 1996b). It has a period of 0.58 days. This star is likely to be the variable CL Boo identified photographically by Romano (1979), who listed it as a possible RR Lyrae variable with the original designation GR 299. The reported coordinates and those listed in the Combined General Catalogue of Variable Stars (Kholopov et al. 1998)[2] are 2.′6 off; however, our star, 2-6-0264, matches the reported magnitude and is the only RR Lyrae star we found in the field.

Other classes of pulsating variables that might be found in these data include the γ Doradus and rapidly oscillating Ap (roAp) stars. The γ Doradus class varies via *g*-mode pulsations with one or more periods between 0.4 and 3 days and amplitudes of $V \lesssim 0.1$. These stars are found among spectral types A7–F5 and luminosity classes V–IV, placing them on the H-R diagram near the red edge of the δ Scuti instability strip (Kaye et al. 1999). The typical amplitudes of γ Doradus stars are detectable for the bright stars in our survey and should show periodic variations. We inspected the periodic light curves but

[2] See http://vizier.u-strasbg.fr/cgi-bin/VizieR/?-source=II/214.

TABLE 3
SELECTED VARIABLE STARS

Identification Number	Figure[a]	Classification
1-1-0298	5*a*	SX Phe/δ Scuti
1-1-0645	5*b*	SX Phe/δ Scuti
1-1-0711	5*c*	SX Phe/δ Scuti
1-1-0838	5*d*	SX Phe/δ Scuti
1-3-1194	5*e*	SX Phe/δ Scuti
1-1-1299	5*f*	SX Phe/δ Scuti
1-8-0323	5*g*	SX Phe/δ Scuti
1-7-0503	6*c*	SX Phe/δ Scuti
1-5-0502	6*d*	SX Phe/δ Scuti
1-5-0832	6*e*	SX Phe/δ Scuti
1-7-0998	6*f*	SX Phe/δ Scuti
1-5-1202	6*g*	SX Phe/δ Scuti
2-7-0122	6*a*	SX Phe/δ Scuti
2-6-0264	6*b*	RR*ab* (CL Boo)
1-1-0033	7*a*	EA
1-4-1044	7*b*	EW
1-2-0950	7*c*	EW
1-4-1128	7*d*	EA
1-3-1223	7*e*	EW
1-7-0089	7*f*	EW
1-6-0237	7*g*	EA
1-5-1217	7*h*	EA
1-4-0082	8*a*	Unknown
1-6-0395	8*b*	Unknown
1-2-0442	8*c*	Unknown
1-1-0568	8*d*	Unknown
1-1-0949	8*e*	Unknown
1-4-1145	8*f*	Unknown
1-4-1316	8*g*	Unknown
1-3-1460	8*h*	Unknown
2-4-0188	11*a*	Unknown
1-3-1466	11*b*	Unknown

[a] Refers to the corresponding figure number and panel showing the light curve.

found no definitive γ Doradus candidates. Those variables with periods in the 0.4–3 day range are either identified as eclipsing stars or remain unclassified, but the possibility exists that one or more is a γ Dor star (see § 3.7). The roAp stars are characterized by short-period (5–20 minutes), low-amplitude (few millimagnitudes) pulsations found among chemically peculiar members of the B8–F0 spectral and V–VI luminosity classes (Matthews 1991). Our time sampling rate makes it difficult to detect such short-period variables; in fact, we limit our period search to 12 minutes and longer (twice the light-curve sampling time). No periodic variables with periods between 12 and 20 minutes are found.

In Figures 1*d* and 2*d* we plot the fraction of all stars identified as pulsating variables versus $B-V$ and $V-I$, respectively. The pulsating stars are relatively blue compared to the color distribution of variables of all types. We can use these statistics to determine the contribution of pulsating stars to the total number of variable stars at these colors and the fraction of all stars at these colors that are identified as pulsating stars. Because the majority of pulsating stars we find are bright and their amplitudes of variability are low, we take as our sample those stars brighter than $V = 16.5$. We find that 12 of our 14 pulsating stars have $V < 16.5$. Of those 12, 11 fall in the color range $0 < B-V < 0.6$ and seven fall in the color range $0.2 < V-I < 0.6$. In total, we find 89 stars with $0 < B-V < 0.6$ and $V < 16.5$, 19 of which are variable, and 613 stars with $0.2 < V-I < 0.6$ and $V < 16.5$, 44 of which are variable. Thus, in the color range $0 < B-V < 0.6$, pulsations account for 58% of the bright variable stars and 12% of all of the bright stars are identified as pulsating variables. Similarly, in the color range $0.2 < V-I < 0.6$, pulsations account for 16% of the bright variable stars and 1% of all of the bright stars are identified as pulsating variables. The fraction of stars in the δ Scuti instability strip that pulsate has been estimated at one-third to one-half (Breger 2000). This suggests that more pulsating stars would be found (with lower amplitudes) as we look at large samples of stars with increasingly good precision.

3.6. Eclipsing Variables

We identify and classify variables as eclipsing by visually inspecting the light curves. In most cases, periodic primary and/or secondary eclipses are seen on multiple nights. In a few cases, only a single eclipse is seen for an otherwise nonvarying star. The signature of an eclipse is normally distinguished from other stellar variations provided that the depth of the eclipse exceeds the noise of the light curve by a significant amount. Therefore, the brightest eclipsing variables are easily classified, while fainter ones may be unclassified. In total, we positively identify 17 stars as eclipsing variables. This is ~8% of the 222 total variable stars found.

Light curves of selected eclipsing variables are shown in Figure 7, and additional information for these stars is given in Table 3.

Figures 1*e* and 2*e* show the fraction of all stars identified as eclipsing variables as a function of $B-V$ and $V-I$, respectively. The majority of the eclipsing variables have (composite) colors that correspond to F–K stars. These distributions can be compared with those of the variable fraction for all types of variability shown in Figures 1*a* and 2*a*. The eclipsing variables have a color distribution that is indistinguishable from the aggregate of stars in the survey.

3.7. Unclassified Variables

Most (86%) of the variables we found could not be positively identified as eclipsing, pulsating, or another recognizable class. Some of these stars may be eclipsing or pulsating variables, but the signal-to-noise ratio, time sampling, or other limitations of this data set were insufficient to identify them. However, other classes of variable stars are present in these data and are important contributors to the variable fraction.

In Figure 8 we plot the light curves of eight unclassified variable stars. The light curves in Figures 8*b*, 8*f*, and 8*e* vary periodically with periods less than 1 day. These stars are probably

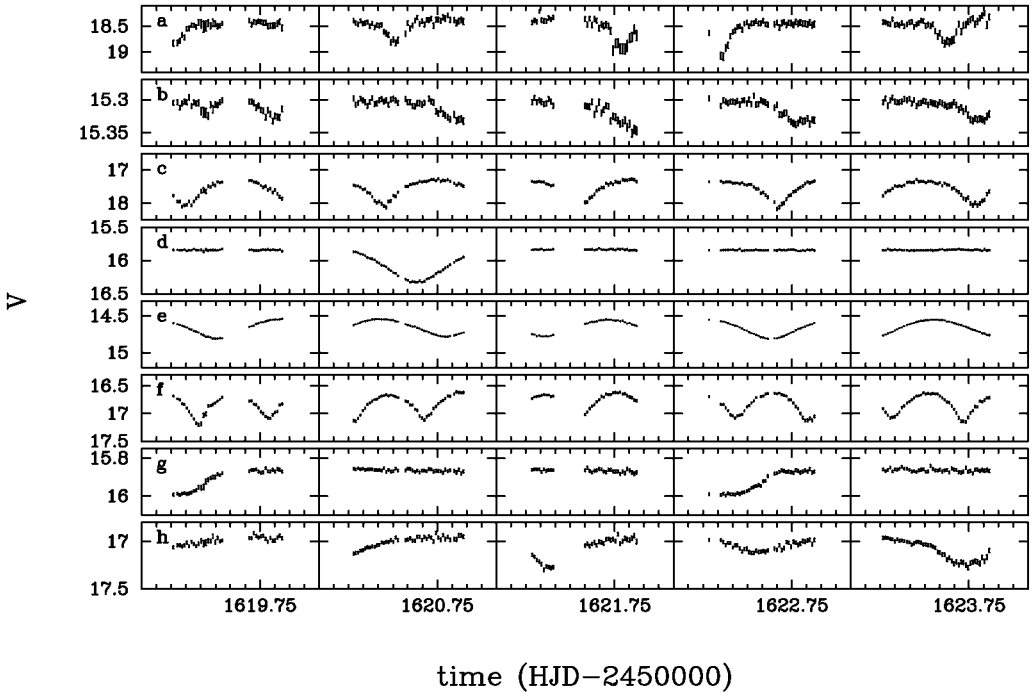

FIG. 7.—Sample light curves representing eight eclipsing variables found in Field 1. See legend of Fig. 5 for details.

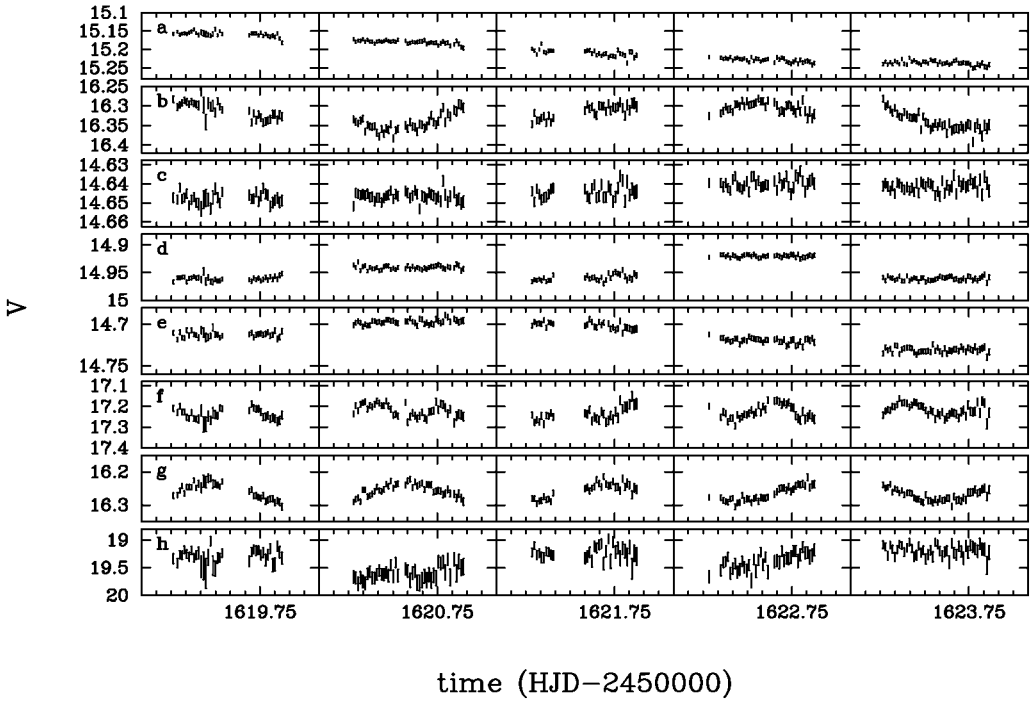

FIG. 8.—Sample light curves representing eight unclassified variables found in Field 1. See legend of Fig. 5 for details.

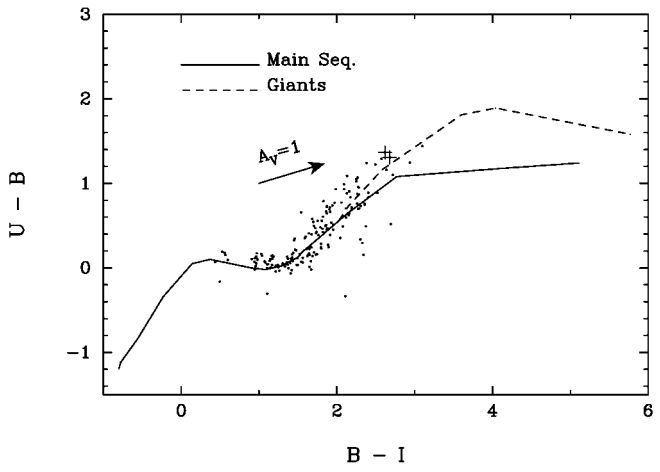

FIG. 9.—Points represent $U-B$ and $B-I$ colors for all variable stars in both fields. The plus signs represent two stars likely to be giants (see § 3.8). The solid line shows the location of the main sequence, and the dashed line shows the location of the giant branch given by Cox (2000). An arrow indicates the direction of interstellar reddening for the $R_V = 3.1$ extinction curve of Mathis (1990).

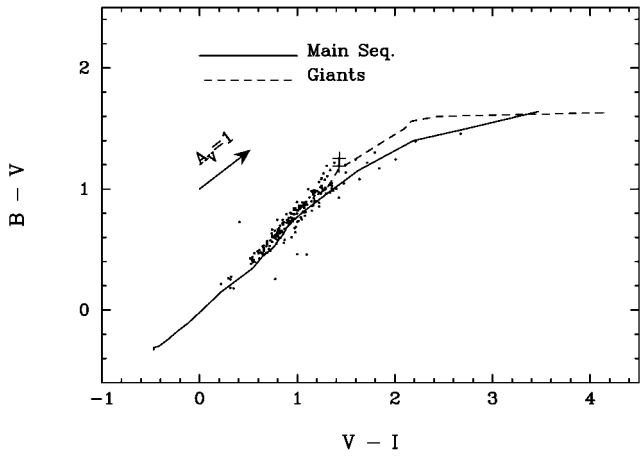

FIG. 10.—Same as Fig. 9 but for $B-V$ and $V-I$ colors.

eclipsing or pulsating variables, but which type is unclear. The star 1-6-0395 (Fig. 8*b*) has a period of 0.44 days and an amplitude of $\Delta V \simeq 0.075$ and represents the best example of a star that has a period consistent with the γ Dor class (see § 3.5).

Light curves that show mainly night-to-night variations like those in Figures 8*a*, 8*c*, 8*d*, and 8*e* are common in our data and represent the majority of the variables found. Many, including these four examples, have colors of late G or K stars.

Chromospheric activity can induce photometric variations in late-type dwarfs and giants as active regions are rotated toward and away from the observer with the period of stellar rotation. A large sample of such stars was observed by Strassmeier et al. (1989), who present light curves and period analyses for these stars. Most were young and rapidly rotating or close binaries in which tidal forces have synchronized the rotational and orbital periods. The unidentified variable stars in our survey with night-to-night variations, but little variation seen within single nights, are likely to be spotted variables or pulsating stars with periods longer than 1 week.

3.8. Variable Giants

The *UBVRI* colors of stars can provide some indication of luminosity class. In certain cases (K or later), giants are identifiable by their broadband colors, allowing us to examine variability in giants. We plot the colors of our variable stars in Figures 9 and 10. The variables plotted are those in which the random error from Poisson noise fluctuations in each color is less than 0.1 mag. The colors for MK spectral types calibrated by Cox (2000) are shown with a solid line for the main sequence and a dashed line for giants. The reddening vector associated with an extinction of $A_V = 1$ is also shown. In total, five stars (variables and nonvariables) are found to have precise colors and locations in these plots that place them far from the main sequence with the colors of early K giants. Two of these stars are variables and are represented by the plus signs in Figures 9 and 10. Given the uncertainties in comparing colors between different broadband filter systems, the intrinsic scatter found for the colors of all of our stars, and the small separation in color between the main sequence and giant branch in the G and early K spectral classes, a foolproof identification of luminosity class is not possible for these stars (they might be giants). The two-color diagrams do show that for later spectral types (K3–M), the color separation between dwarfs and giants is greater, making luminosity classification easier. Furthermore, the effects of reddening do not cause any ambiguity when we assign luminosity classes to the giants we identified.

The light curves for our two variable giants are shown in Figure 11. Both exhibit ~1% variations on a day-to-day timescale. We searched these light curves for evidence of intranight variability by our χ^2 value for a constant-fit test (see § 3.3) applied to individual nights. Star 1-3-1466 in Figure 11*b* shows a ~6 mmag variation within the fourth night of data.

Long-term monitoring of a sample of G, K, and M0 field giants has shown that low-amplitude variations (a few millimagnitudes) exist in a large fraction of these giants on timescales ranging from days to weeks. Henry et al. (2000) found that 100% of the K5 and later type giants in a large sample were variable, 19% of G6–G9 giants were variable (the least variable spectral classes), and then the percentage of variables increased once again toward earlier types. These variations were identified as pulsations. It is likely that pulsations play a significant role in the variable giants identified in our survey, but observations that combine both short-term (minutes) and long-term (weeks) time sampling would allow us to determine the precise nature of their variability.

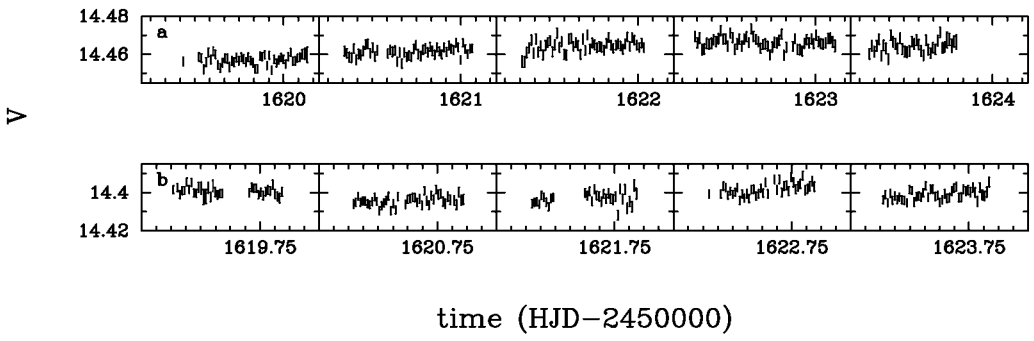

FIG. 11.—Light curves representing two giant variables found in our survey. See legend of Fig. 5 for details.

4. DISCUSSION AND CONCLUSION

We have presented statistics on and individual examples of variables found in a *V*-band time-series survey of field stars. The magnitude range of this survey ($13.8 < V < 19.5$) selects mostly solar-like stars but also a few higher mass stars, later type dwarfs, and giants. An analysis of the fraction of stars in which variability is detected shows that relatively few stars with solar-like colors are variable but that stars bluer than the Sun are variable at a high percentage. A secondary peak in the variability fraction is seen in stars redder than the Sun.

Pulsating stars such as those in the δ Scuti and/or SX Phe classes account for at least 16% and 58% of the blue variables in the color ranges $0.2 < V-I < 0.6$ and $0 < B-V < 0.6$, respectively. The excess of blue stars that are variable (the blue peak in variable fraction) may be entirely attributable to pulsating stars, but not all can be identified unambiguously. A total of 17 eclipsing variables is positively identified (8% of the variable total); however, many of the unclassified variables are probably eclipsing binaries. Eclipsing variables apparently contribute to the variable fraction over a wide range in color.

The level and characteristics of the variability observed, especially in the unclassified stars, are not unexpected. As one observes later spectral types (G–M), the amount of variability due to starspots, chromospheric activity, rotation effects, and magnetic fields increases. For late-type giants, pulsation (especially multiperiodic modes), mass loss, and cool, low-gravity atmospheric effects give rise to variability as well. Of particular interest is how observational projects aimed at detecting extrasolar planetary transits will be able to distinguish between real transits and other phenomena (e.g., grazing stellar eclipses, active regions of the chromosphere that rotate in and out of view). Nonperiodic variations with a duration similar to that of a transiting planet may seem periodic when observed over a short time interval or with limited photometric precision. At photometric precisions near 1 mmag, at least ~17% of all field stars are variable. At the precisions used for transit searches, this percentage is likely to increase. An understanding of the true nature of variable stars through long-term monitoring and detailed observational follow-up of a representative sample, as well as development and comparison to models, is required to properly perform a search for extrasolar planets.

Identifying stars that exhibit constant photometric behavior is another use for our survey database. Stars that exhibit no statistically significant change in flux on a night-to-night basis are of interest as potential calibrators for high-precision photometric or astrometric surveys.

Upcoming space astrometry missions such as the *Space Interferometer Mission* (*SIM*) require stars whose photocenters are constant to microarcsecond scales. *SIM* is investigating K giants at $V \simeq 12$ as potential reference objects (Frink et al. 2001). Such stars will have an apparent size of ~100 μas (van Belle 1999), requiring photocentric consistency to better than 1 part in 100. Stellar photocenters can shift as a result of binary motion (Wielen 1996), color changes during pulsation, and changes in spots and ejecta in the photosphere. The most extreme examples of objects that are both photometric and astrometric variables are the Mira variables found within the *Hipparcos* database (Whitelock & Feast 2000); for these objects, milliarcsecond motions of their photocenters are accompanied by photometric variability of 2–10 mag in the visible. Establishing long- and short-term photometric consistency to 0.1 mmag for particular categories of stars will help identify prime reference candidates for *SIM* and other missions. Establishing broad photometric and astrometric behavior characteristics of giants is beyond our currently limited sample of candidates. However, the high percentage of these objects that exhibit low-level variations (40%) is a provocative incentive to expand our investigation of giants, particularly as they impact upcoming missions.

The authors wish to thank Don Walter and Charles McGruder for their interest and support of this research. We also thank the referee for insightful comments on improving this manuscript. This work was supported in part through South Carolina State University by NASA/MU-SPIN NCC 5-534 and NASA/OSS NAG 5-10145 and through NASA grant NAG 5-8762 to Western Kentucky University. S. B. H. received partial support for this work from NASA Origins/JPL grant 1225196.

REFERENCES

Adelman, S. J. 2001, A&A, 367, 297
Akerlof, C., et al. 2000, AJ, 119, 1901
Albrow, M. D., Gilliland, R. L., Brown, T. M., Edmonds, P. D., Guhathakurta, P., & Sarajedini, A. 2001, ApJ, 559, 1060
Alcock, C., et al. 1995, AJ, 109, 1653
Bahcall, J. N., & Soneira, R. M. 1980, ApJS, 44, 73
Bauer, F., et al. 1999, A&A, 348, 175
Borucki, W. J., Caldwell, D., Koch, D. G., Webster, L. D., Jenkins, J. M., Ninkov, Z., & Showen, R. 2001, PASP, 113, 439
Breger, M. 1980, ApJ, 235, 153
———. 2000, in ASP Conf. Ser. 210, Delta Scuti and Related Stars, ed. M. Breger & M. Montgomery (San Francisco: ASP), 3
Brown, T. M., & Charbonneau, D. 2000, in ASP Conf. Ser. 219, Disks, Planetesimals, and Planets, ed. F. Garzón, C. Eiroa, D. de Winter, & T. Mahoney (San Francisco: ASP), 584
Cox, A. N. 2000, Allen's Astrophysical Quantities, ed. A. Cox (4th ed.; New York: Springer)
Everett, M. E., & Howell, S. B. 2001, PASP, 113, 1428 (EH)
Eyer, L., & Grenon, M. 1997, in Proc. ESA Symp. *Hipparcos*: Venice '97, ed. B. Battrick (ESA SP-402; Noordwijk: ESA), 467
Feast, M. W. 1996a, in Light Curves of Variable Stars, ed. C. Sterken & C. Jaschek (Cambridge: Cambridge Univ. Press), 81
———. 1996b, in Light Curves of Variable Stars, ed. C. Sterken & C. Jaschek (Cambridge: Cambridge Univ. Press), 83
Frink, S., Quirrenbach, A., Fischer, D., Roser, S., & Schilbach, E. 2001, PASP, 113, 173
Gautschy, A., & Saio, H. 1996, ARA&A, 34, 551
Hearnshaw, J. B., Bond, I. A., Rattenbury, N. J., Noda, S., & Takeuti, M. 2000, in ASP Conf. Ser. 203, The Impact of Large-Scale Surveys on Pulsating Star Research, ed. L. Szabados & D. N. Kurtz (San Francisco: ASP), 31
Henry, G. W., Fekel, F. C., Henry, S. M., & Hall, D. S. 2000, ApJS, 130, 201
Kaye, A. B., Handler, G., Krisciunas, K., Poretti, E., & Zerbi, F. M. 1999, PASP, 111, 840
Kholopov, P. N., et al. 1998, Combined General Catalogue of Variable Stars (VizieR On-line Data Catalog II/214A)
Koch, D. G., Borucki, W., Webster, L., Dunham, E., Jenkins, J., Marriott, J., & Reitsema, H. J. 1998, Proc. SPIE, 3356, 599
Landolt, A. U. 1992, AJ, 104, 340
Mallen-Ornelas, G., et al. 2001, BAAS, 199, 66.02
Matthews, J. M. 1991, PASP, 103, 5
Mathis, J. S. 1990, ARA&A, 28, 37
Mochejska, B. J., Stanek, K. Z., Sasselov, D. D., & Szentgyorgyi, A. H. 2002, preprint (astro-ph/0201244)
Monet, D., et al. 1998, USNO-A2.0: A Catalog of Astrometric Standards (Washington, DC: USNO)
Pojmański, G. 2000, Acta Astron., 50, 177
Poretti, E. 2000, in Variable Stars as Essential Astrophysical Tools, ed. C. Ibanoglu (Dordrecht: Kluwer), 227
Press, W. H., Teukolsky, S. A., Vetterline, W. T., & Flannery, B. P. 1992, Numerical Recipes in FORTRAN 77: The Art of Scientific Computing (Cambridge: Cambridge Univ. Press)
Romano, G. 1979, Inf. Bull. Variable Stars, 1674
Roun, D., et al. 1999, Phys. Chem. Earth C, 24, 567
Strassmeier, K. G., Hall, D. S., Boyd, L. J., & Genet, R. M. 1989, ApJS, 69, 141
Street, R. A., et al. 2000, in ASP Conf. Ser. 219, Disks, Planetesimals, and Planets, ed. F. Garzón, C. Eiroa, D. de Winter, & T. Mahoney (San Francisco: ASP), 572
Tody, D. 1986, Proc. SPIE, 627, 733
van Belle, G. T. 1999, PASP, 111, 1515
Whitelock, P., & Feast, M. 2000, MNRAS, 319, 759
Wielen, R. 1996, A&A, 314, 679
Żebruń, K., et al. 2001, Acta Astron., 51, 317